ADVANCED FUNCTIONAL MATERIALS
www.afm-journal.de

Carbon-Based Anodes for Lithium Sulfur Full Cells with High Cycle Stability

*Jan Brückner, Sören Thieme, Falko Böttger-Hiller, Ingolf Bauer, Hannah Tamara Grossmann, Patrick Strubel, Holger Althues, Stefan Spange, and Stefan Kaskel**

The lithium sulfur battery system has been studied since the late 1970s and has seen renewed interest in recent years. However, even after three decades of intensive research, prolonged cycling can only be achieved when a large excess of electrolyte and lithium is used. Here, for the first time, a balanced and stable lithium sulfur full cell is demonstrated with silicon–carbon as well as all-carbon anodes. More than 1000 cycles, a specific capacity up to 1470 mAh g^{-1}_{sulfur} (720 mAh $g^{-1}_{cathode}$), and a high coulombic efficiency of over 99% even with a low amount of electrolyte are achieved. The alternative anodes do not suffer from electrolyte depletion, which is found to be the main cause of cell failure when using metallic lithium anodes.

1. Introduction

The lithium sulfur battery system is a promising candidate for high energy storage devices beyond the lithium ion technology. Sulfur is nontoxic, abundant and offers a theoretical capacity of 1672 mAh g^{-1}_{sulfur} that exceeds current cathode material by almost one order of magnitude. Even conservative approximations predict lithium sulfur batteries to achieve twice the gravimetric energy density of lithium ion batteries at cell level. At the same time the material costs for a lithium sulfur battery will most likely be drastically lower than in lithium ion batteries by replacement of expensive cathode materials. However, the biggest drawback that has so far prevented lithium sulfur from commercialization is the low cycle stability.

Since sulfur is an insulator it has to be in intimate contact with a conducting matrix, commonly carbon. High energy densities can only be achieved when the sulfur loading as well as the sulfur utilization is maximized.

J. Brückner, S. Thieme, I. Bauer, H. T. Grossmann, P. Strubel, Dr. H. Althues, Prof. S. Kaskel
Fraunhofer Institute for Material and Beam Technology (IWS)
Winterbergstraße 28, 01277, Dresden, Germany
E-mail: stefan.kaskel@chemie.tu-dresden.de
Dr. F. Böttger-Hiller, Prof. S. Spange
Chair Polymer Chemistry
Chemnitz University of Technology
Straße der Nationen 62, 09111, Chemnitz, Germany
Prof. S. Kaskel
Chair Inorganic Chemistry I
Dresden University of Technology
Bergstraße 66, D-01062, Dresden, Germany

DOI: 10.1002/adfm.201302169

In recent years major improvements were made by employing advanced carbon materials that encapsulate sulfur and suppress the polysulfide shuttle mechanism.[1–8] However, rarely more than 100 cycles are reported. One reason behind this is the widespread use of lithium metal as the anode. Liquid electrolytes known to date are unstable versus metallic lithium and do not form a stable solid electrolyte interface (SEI). Similar to the lithium oxygen cell,[9] prolonged cycling can only be achieved when an excessive amount of both electrolyte and lithium is used.[4,10–12] Therefore the calculation of energy densities and the evaluation of cycle stability should not solely be based on the sulfur cathode performance.

In general a metallic lithium anode has major drawbacks. Dendrite formation and the low melting point may result in thermal runaway and cause serious safety concerns.

It shall be noted that dendrite formation in a lithium sulfur battery is an even bigger problem than it is for lithium ion batteries. Unlike lithium ion, intermediate dis-/charge products (lithium polysulfides) are formed that are soluble in the electrolyte and thus in direct contact with the anode material. As a result, active material is lost when a new SEI is formed on dendritic lithium. Lithium nitrate ($LiNO_3$) has been reported as an electrolyte additive to circumvent this problem by forming a more stable SEI.[13,14] The passivation is based on an oxidation of solid lithium-sulfur species covering the anode. However the additive does only delay the degradation since $LiNO_3$ is continuously consumed by the passivation of new dendrites.

This problem can be masked using an extreme excess of electrolyte. Only very few publications mention the amount of electrolyte added to the cell.[15] In a recent paper, Zhang showed that an electrolyte/sulfur ratio below 10 µL mg^{-1}_{sulfur} significantly shortens the cycle life when metallic lithium is used as the anode.[16]

Zhang also showed that $LiNO_3$ decomposes below 1.6 V.[17] If an excess of electrolyte (equals a high quantity of $LiNO_3$) is present, discharging below 1.6 V can be repeated several times before the coulombic efficiency decreases and $LiNO_3$ is depleted. However, this capacity is irreversible and should not be attributed to sulfur.[10]

Energy densities are commonly calculated by the capacity of the cathode. Usually at least 250 µm thick lithium anodes are used for testing. Assuming a cathode loading of 1.5 mg_{sulfur} cm^{-2} and a high sulfur utilization of 72% (1200 mAh g^{-1}_{sulfur}), the

areal capacity is 1.8 mAh cm^{-2}. A 250 µm thick lithium foil corresponds to 13.4 mg_{Li} cm^{-2} or 50.7 mAh cm^{-2}. Accordingly the excess of lithium is in fact more than 2700%. Most publications use a sulfur loading that is even lower than 1.5 mg_{sulfur} cm^{-2}[4,10,11,18–20] or an lithium foil thicker than 250 µm.[11]

The problems of balancing the anode and cathode, as well as the safety concerns regarding metallic lithium, have resulted in investigations of alternative cell concepts. Three different approaches where published. Scrosati and co-worker published a tin anode versus a lithium sulfide cathode,[21] Cui's group used a silicon anode and lithium sulfide cathode,[22] and a prelithiated silicon anode in combination with a sulfur cathode was published by Aurbach and co-workers.[23]

All of those concepts proof that a full cell can be realized with the lithium sulfur cell chemistry. However, the reported cycle stability was not satisfactory and the observed degradation can still largely be attributed to an instable anode. Here we report, for the first time, a balanced and stable lithium sulfur full cell with silicon–carbon and all-carbon anodes achieving more than 1000 reversible cycles.

2. Results and Discussion

2.1. Flexible Si-C anode

Inspired by the pioneering work of Aurbach and co-workers[23] we sputtered 4 µm of amorphous silicon (0.95 mg cm^{-2}). But instead of using roughened copper foil as the substrate we used a flexible carbon fiber material (**Figure 1**). Due to the 3D structured substrate of the final layer thickness of amorphous silicon was around 1 µm (S1).

For the Si–C anode 300 cycles of reversible de-/lithiation were achieved at elevated dis-/charge rates of 2 A $g^{-1}_{silicon}$ in a half cell setup (**Figure 2**a). The cycle stability was enhanced

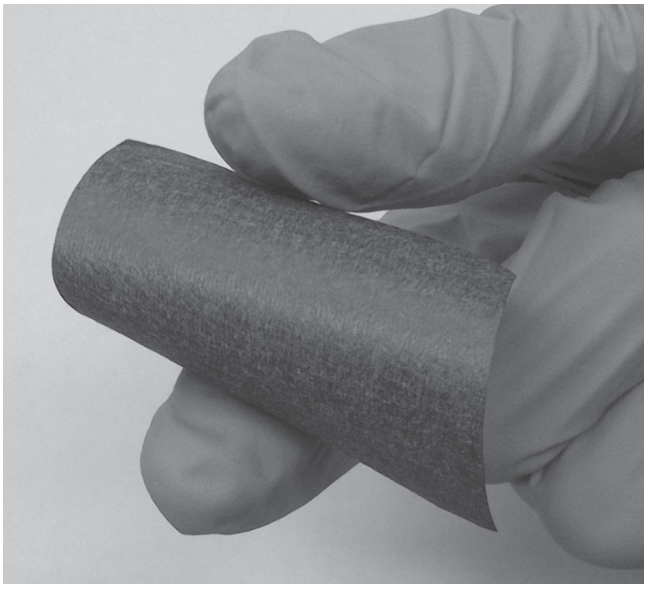

Figure 1. Photograph of a-Si coated carbon non-woven (silicon layer thickness < 1 µm, 0.95 $mg_{silicon}$ cm^{-2}).

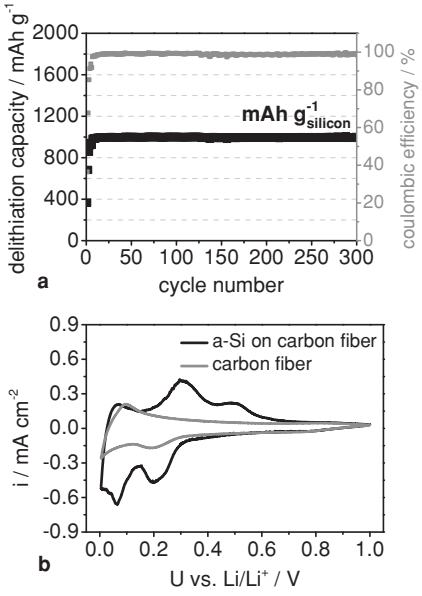

Figure 2. (a) Delithiation capacity of the anode (black) and coulombic efficiency (gray) at a dis-/charge current of 2 A $g^{-1}_{silicon}$ (1.9 mA cm^{-2}). The lithiation capacity was limited to 1000 mAh $g^{-1}_{silicon}$. Due to SEI formation the delithiation capacity and coulombic efficiency is lowered in the first cycles. (b) Cyclic voltammetry at a scan rate of 20 µV s^{-1} shows the cathodic peaks at 0.21 and 0.07 V as well as the anodic peaks at 0.31 and 0.50 V for amorphous silicon. The anodic peak at around 0.1 V can be attributed to lithium extraction from the carbon fiber.

when lithiation was limited to 1 Ah $g^{-1}_{silicon}$ (0.95 mAh cm^{-2}). This is consistent with literature where a limitation of lithiation results in an improved cycle stability.[24,25] The electrolyte was 1 M LiTFSI, 0.25 M $LiNO_3$ in 1,2-dimethoxy ethane (DME)/1,3-dioxolane (DOL) (1:1 by volume). The dis-/charge current was 0.4 A $g^{-1}_{silicon}$ for five formation cycles. In the following cycles the half cells were dis-/charged at 2 A $g^{-1}_{silicon}$. This is equivalent to a dis-/charge time of 30 min.

The high cycle stability may also be attributed to the electrolyte. It was recently reported that $LiNO_3$ and DOL significantly improve the cycle stability of silicon based anodes by forming a more stable SEI.[26] Fully lithiated, however, the Si–C composite anode shows degradation as well as a lowered coulombic efficiency after the 35th cycle (S2).

Further investigation, revealed that part of the capacity is derived from the carbon substrate (Figure 2b). Besides the typical delithiation peaks for amorphous silicon at 0.21 and 0.07 V,[23] a peak at 0.1 V is observed versus metallic lithium. It is known that carbonized polyacrylonitrile (PAN) fibers deliver reversible capacity.[27,28] However previous tests were done in carbonate-based electrolytes and without lithium polysulfides. Ethers were previously only investigated as additives for carbonate solutions that lower the viscosity of the electrolyte.

To utilize the relatively high rate capability of the Si–C anode (1.9 mA cm^{-2}, 30 min discharge) a conductive carbon structure is required as the sulfur host material. Moreover, a highly accessible porosity allowing for fast lithium ion diffusion is required for the cathode to work at high current densities.

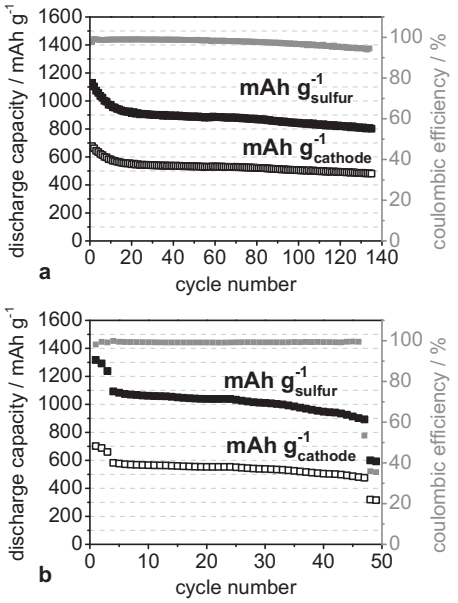

Figure 3. (a) Discharge capacity (black) and coulombic efficiency (gray) of sulfur cathode in a half cell setup. The dis-/charge current is 167 mA g^{-1}_{sulfur}. Reversible dis-/charging is obtained for 135 cycles. (b) Discharge capacity (black) and coulombic efficiency (gray) of sulfur cathode in a half cell setup. The dis-/charge current is 167 mA g^{-1}_{sulfur} for three formation cycles and 836 mA g^{-1}_{sulfur} in the subsequent cycles. Cell failure is observed in cycle 47.

Archer et al. and Gao et al. recently demonstrated that hollow carbon spheres fulfill these requirements since they offer high sulfur utilization, polysulfide retention as well as a very good rate capability.[2,3]

Thus we used hollow carbon spheres specially tailored for the application in lithium sulfur cells. The synthesis procedure for those spheres is reported elsewhere.[29,30] Sulfur was melt infiltrated over night at 155 °C into the carbon matrix (sulfur to carbon ratio 2:1 by weight). The cathode was prepared by mixing 80 wt% of the carbon–sulfur composite with 10 wt% polytetrafluoroethylene (PTFE) and 10 wt% multi-walled carbon nanotube (MWCNT) conductive additive. This resulted in a cathode with an active material content (sulfur) of 53.3 wt%. The areal loading was 1.64 mg_{sulfur} cm^{-2}. A more detailed description of the cathode preparation and cell assembly was recently published by our group.[6]

When the cathode was cycled in a half cell setup versus elemental lithium at 167 mA g^{-1}_{sulfur} we were able to achieve reversible cycling for 135 cycles (**Figure 3**a). However, when the same cathode was cycled at 836 mA g^{-1}_{sulfur} (after three formation cycles at 167 mA g^{-1}_{sulfur}) the half cell failed rather quickly after 45 cycles (Figure 3b). We attribute this phenomenon not only to pronounced dendrite formation but also to rapid electrolyte depletion. It is documented that the dendrite formation is more pronounced at higher current densities.[31] According to Xiong et al. a compact and smooth surface film is formed after several hours, when a metallic lithium electrode is immersed in a $LiNO_3$ containing electrolyte.[32] If, in contrast, the time between subsequent charge–discharge cycles is short,

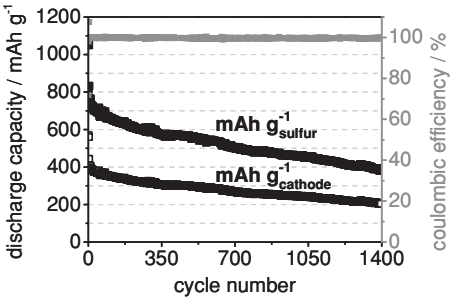

Figure 4. Discharge capacity (black) and coulombic efficiency (gray) of the full-cell setup. The dis-/charge current is 167 mA g^{-1}_{sulfur} for three formation cycles and 836 mA g^{-1}_{sulfur} (1.37 mA cm^{-2}) in the subsequent cycles. The discharge capacity was 765 mAh g^{-1}_{sulfur} in the 5th cycle and faded only 0.08% afterwards. The coulombic efficiency was 99.8% even in the 1390th cycle.

no compact protection layer is formed. As a result lithium may predominantly react with the solvents of the electrolyte. Since our amount of electrolyte is rather low (12 µL mg^{-1}_{sulfur}), depletion may occur earlier than in other cell setups. Therefore, we expect that the metallic lithium anode is the major reason for the low cycle stability predominantly at elevated dis-/charge rates. It should be noted that a higher coulombic efficiency is observed at higher currents for the half cell setup. This may be attributed to the hindered diffusion of lithium polysulfides due to shorter dis-/charge times.[33]

To assemble a full cell the Si–C anode was lithiated by short circuiting versus metallic lithium. The pre-lithiated anode was afterwards transferred and assembled with the carbon-sulfur cathode. The amount and type of electrolyte for the full cell was the same as for all half cell tests. After three formation cycles at a current rate of 167 mA g^{-1}_{sulfur}, the current was increased to 836 mA g^{-1}_{sulfur} for the following dis-/charge cycles. In contrast to the half cell, the full cell showed a good stability at 836 mA g^{-1}_{sulfur} and did not fail after 45 cycles due to electrolyte depletion and/or dendrite formation (S3). In fact more than 1300 reversible cycles were achieved with this setup (**Figure 4**). The discharge capacity was 765 mAh g^{-1}_{sulfur} in the 5th cycle and faded extremely slowly (~0.08%) over the following cycles. Even in the 1390th cycle the coulombic efficiency was at 99.8%. It should also be noted that the excess of lithium in this full cell was only 60%. We therefore attribute the enhanced cycle stability to the fact that a stable SEI is formed and the electrolyte is not consumed upon cycling.

Although our new approach clearly demonstrates the numerous advantages of the full cell concept, one drawback might be the decrease in energy density. The electrochemical potential of lithiated silicon is higher than that of elemental lithium. As a result the average cell voltage of the presented full cell is lowered by 0.24 V to 1.89 V (S4).

2.2. All-Carbon Anodes

The carbon fibers were investigated in more detail by X-ray diffraction (**Figure 5**). Graphite (MCMB) produces a distinctive peak (002) at $2\theta = 26.5°$ corresponding to the interlayer spacing

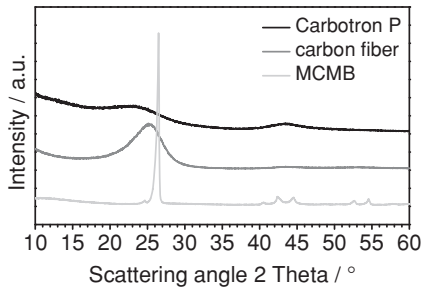

Figure 5. XRD patterns for commercial hard carbon (Carbotron P), carbon fiber and graphite (MCMB). The peak attributable to the 002 graphite reflex corresponds to the average interlayer spacing.

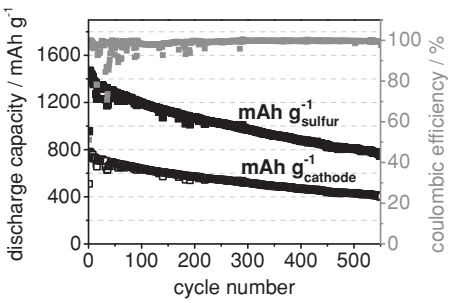

Figure 6. Discharge capacity (black) and coulombic efficiency (gray) of the full-cell setup. The dis-/charge current is 334 mA g^{-1}_{sulfur} (0.42 mA cm^{-2}). The discharge capacity was 1355 mAh g^{-1}_{sulfur} (722 mAh $g^{-1}_{cathode}$) in the 10th cycle and faded only 0.08% per cycle. The coulombic efficiency was at 99.1% even in the 550th cycle.

of the graphene sheets (0.335 nm for crystalline graphite). In contrast, the carbon fibers show a broad peak at $2\theta = 25.1°$ (d = 0.353 nm) which is characteristic for non-graphitic carbons.[34] Cross-links between smaller domains of graphene stacks result in micropores that increase the average interlayer spacing. As the carbon fibers are carbonized at very high temperatures they are non-graphitizable.[28]

For comparison commercial non-graphitizable carbons (hard carbons) were tested as alternative anode materials (CP-anode) in the lithium sulfur battery. The peak for hard carbons is at $2\theta = 23.1°$ (0.385 nm) indicating an even wider average interlayer spacing compared to the carbon fiber. Due to the existing cross-links the CP-anode shows an extraordinary stable cycling behavior in the ether based electrolyte (S5). No delamination is observed, which prevents the usage of graphite in ether based electrolytes.

A hard carbon containing slurry was coated on and pressed into the carbon fiber network to lower the porosity of the carbon fibers and increase the areal capacity (S6). For the full cell testing the all-carbon anode was prelithiated versus metallic lithium.

It was also found that the sulfur utiliziation can be increased when the CNT/PTFE ratio in the cathode is adjusted. While sulfur loading and porous carbon content where unchanged, the ratio was increased from 1:1 to 3:1, which improved the wettability of the cathode. As a result, the sulfur utilization was increased by 26% to 1658 mAh g^{-1}_{sulfur} (99.2% utilization) for the first cycle (S7). In a half cell setup, a cathode comprising the 3:1 ratio was dis-/charged at 334 mA/g_{sulfur} (0.45 mA cm^{-2}) versus metallic lithium. The amount of electrolyte was 13 µL mg^{-1}_{sulfur}. With 168 reversible cycles, the cycle stability of the cathode with 3:1 CNT:PTFE ratio was very high and comparable to the sample with 1:1 ratio in a half cell setup.

The full cell was dis-/charged at 334 mA g^{-1}_{sulfur} (0.42 mA cm^{-2}), 14 $\mu L_{electrolyte}$ mg^{-1}_{sulfur} and cycled between 1.0 and 2.6 V to account for the potential of the carbon anode (S8). The increased sulfur utilization (2nd cycle: 1471 mAh g^{-1}_{sulfur}, 784 mAh $g^{-1}_{cathode}$) for the 3:1 ratio was reproduced in the full cell setup (**Figure 6**). This is especially noteworthy since the cell was balanced and the excess of lithium only 10%. Reversible cycling is possible for more than 550 cycles and no cell failure is observed. The capacity fade is again only 0.08% per cycle. Due to the higher sulfur utilization the capacity is 753 mAh g^{-1}_{sulfur} (400 mAh $g^{-1}_{cathode}$) in the 550th cycle. The coulombic efficiency is high at 99.1%. The unsteady behavior, observed for the first cycles, can be reduced when formation cycles are implemented into the testing procedure.

Currently, the amount of electrolyte is still relatively high, which is a limitation of our cell setup. The dead volume in a coin cell results in a minimal amount of electrolyte of 20 µL. We are convinced that the relative amount can be decreased even further in an improved cell type.

The result demonstrates that a hard carbon anode offers superior cycle stability in a lithium sulfur full cell. Using our proposed full cell setup we believe that for the first time it is possible to investigate degradation and aging processes in the lithium sulfur cell without dendrite formation and electrolyte decomposition. One should keep in mind that at high sulfur utilization and at a dis-/charge rate of 334 mA g^{-1}_{sulfur} the cell is cycled for more than five month to achieve 550 cycles. Future work will investigate aging, cathode degradation, and the high-temperature performance of this system.

3. Conclusion

For the first time, we have shown a lithium sulfur battery system delivering reversible capacity for more than 1300 cycles in a full cell setup. The proposed silicon carbon and hard carbon anodes in combination with the dry processed cathodes offer highly improved cycle stability. In a balanced full cell very high sulfur utilization of up to 1470 mAh g^{-1}_{sulfur} (720 mAh $g^{-1}_{cathode}$) in combination with low amount of electrolyte are achieved. The coulombic efficiency is above 99% for more than a thousand cycles and the capacity fade is only 0.08% per cycle. We observed no electrolyte depletion when the silicon carbon or hard carbon anodes were cycled in the lithium sulfur full cell. The cell running dry due to the depletion of electrolyte was found to be the main reason for cell failure in lithium sulfur cells using metallic lithium anodes and a reasonable amount of electrolyte.

This result demonstrates that a hard carbon anode can be used as an alternative anode in the lithium sulfur battery system. For the first time we are able to show that a balanced cell with a minimal lithium excess of 10% is possible. This is a major achievement since literature so far was not able to show

that the lithium sulfur system can achieve reversible cycling below 2000% lithium excess. Our system enables detailed investigations of degradation mechanisms in the lithium sulfur battery system without dendrite formation and electrolyte decomposition.

4. Experimental Section

Synthesis of the Twin Monomer: The synthesis of Tetrafurfuryloxysilan, was carried out according to Grund et al.[35] Tetraethoxysilane (90 mL, 0.4 mol) and furfuryl alcohol (141 mL, 1.6 mol) were mixed, and 0.3 wt% of KOH was added. The mixture was stirred for 3 h at 80 °C and 65 mbar. Then the pressure was reduced over 1 h to 3 mbar and the by-products were distilled off. The product was obtained at 240 °C and 0.4 mbar. Light-yellow crystals precipitated at 0 °C and could be recrystallized from diethyl ether (m.p. 58 °C).

Synthesis of Carbon Spheres: The hollow carbon spheres (HCS) were synthesized according to Böttger-Hiller et al.[29] In a typical polymerization 1.0 g of Aerosil 300 was suspended in 200 mL dichloromethane. Subsequently, 240 mg methanesulfonic acid were given to the suspension and stirred for 15 min at room temperature. After removal of the solvent on an evaporator, the acid-loaded substrate was suspended in 200 mL toluene. 2 g of Tetrafurfuryloxysilan were dissolved in 50 mL toluene and given to the substrate-dispersion. After 30 s the mixture changes its color into brown and the nanocomposite precipitates. After stirring for 15 h at room temperature the brownish solid was filtered off, washed using 100 mL dichloromethane and dried. The coated substrate was heated under argon at a heating rate of 6.2 K/min up to 1100 °C and tempered for 3 h. For removal of the silicon dioxide 10 mL of aqueous hydrofluoric acid (40%) were added to the carbonized material. After three days at room temperature, the resulting HCS were filtered off, washed with water and ethanol and dried.

Tetraethoxysilane, furfuryl alcohol, tetramethoxysilane (98%), methanesulfonic acid (98+%), aqueous hydrofluoric acid (40%), ferric(III)chloride are commercially available products. Aerosil 300 was provided from Degussa. Furfuryl alcohol was distilled immediately before use. The other reagents were used without further purification.

Cathode Preparation: The preparation of the cathode was reported in detail elsewhere.[6] The carbon/sulfur composite was prepared by mixing sulfur (Sigma Aldrich, ≥99.5%) and hollow carbon spheres (HCS) in a weight ratio of 2:1. Sulfur was melt infiltrated at 155 °C for 12 h in air. The cathode was prepared by mixing the carbon/sulfur composite with multi-walled carbon nanotubes (MWCNT, Nanocyl NC 7000 series, 90%) and poly(tetrafluorethylene) (PTFE, ABCR) in a weight ratio of 8:1:1. The sulfur content in the cathode was 53.3 wt%. Under application of shearing forces this mixture was then rolled out at 150 °C. The received sheet was 80 µm thick and laminated onto a carbon-coated, expanded aluminum current collector (Benmetal, 99.5%). The areal loading of sulfur was 1.6–1.8 mg cm^{-2}. Circular electrodes with a diameter of 10 mm (0.79 cm^2) were punched from the cathode sheet. The cathodes with a 3:1 CNT:PTFE ratio were 12 mm in diameter (1.13 cm^2) and the sulfur loading was 1.3–1.5 mg cm^{-2}. All other parameters were the same as for the 1:1 ratio.

Anode Preparation: (1) *a-Si on Carbon Fiber*: The amorphous silicon (0.95 mg cm^{-2}) film was prepared by DC magnetron sputtering of p-doped silicon (99.99%, Robeko) at a pressure of 3×10^{-3} mbar of argon (99.999%) on a commercial carbon non-woven (GDL Y0200, Freudenberg). Circular electrodes with a diameter of 10 mm (0.79 cm^2) were punched from the sheet. (2) *Commercial Hard Carbon on Copper Foil*: A slurry containing 90 wt% hard carbon (Carbotron P, Kureha GmbH), 5 wt% MWCNT and 5 wt% carboxymethyl cellulose (CMC)/styrene-butadiene rubber (SBR) binder (1:1 m/m, 2 wt% in water) was cast onto a 10 µm thick roughened copper foil (SE-Cu58, Schlenk Metallfolien GmbH & Co. KG) by a doctor-blade coating technique. CMC was purchased from MTI Corp. and SBR from Targray. The areal loading was 1.77 $mg_{CarbotronP}$ cm^{-2}. Circular electrodes with a diameter of 12 mm (1.13 cm^2) were punched from the sheet. (3) *Commercial Hard Carbon in Carbon Fiber*: A slurry containing 80 wt% hard carbon (Carbotron P, Kureha GmbH), 5 wt% MWCNT and 15 wt% SBR-binder (15 wt% in water) was pressed into a commercial carbon non-woven (GDL Y0200, Freudenberg). Circular electrodes with a diameter of 12 mm (1.13 cm^2) were punched from the sheet. The electrode weight was 8.62 mg cm^{-2}.

Electrochemical Testing: Coin cells (MTI Corp., CR2016) were assembled in an Argon-filled glove box (MBraun, <0.1 ppm O_2 and H_2O). For half cells metallic lithium (Pi-Kem, 99.0%, diameter 15.6 mm, thickness 250 µm) was used. The electrodes were separated by one layer of a polypropylene separator (Celgard 2500). The electrolyte consisted of 1 M lithium bis(trifluoromethylsulfonyl) imide (LiTFSI, Aldrich, 99.95%), 0.25 M lithium nitrate ($LiNO_3$, Alfa Aesar, 99.98%, anhydrous) in 1,2-dimethoxy ethane (DME, Sigma Aldrich, 99.5%, anhydrous) and 1,3-dioxolane (DOL, Sigma Aldrich, 99.8%, anhydrous). The ratio of the solvents was 1:1 (v/v). The cells were cycled at room temperature with a BaSyTec Cell Test System (CTS). Half cells where cycled between 10 mV and 1 V for silicon-carbon anode, 10 mV to 1.5 V for the all-hard carbon anodes and 1.8 to 2.6 V for cathodes. The cutoff voltage for the full cell with silicon carbon anode was adjusted to 1.5 to 2.6 V to account for the overvoltage of the anode. The full cell with all-hard carbon anode was adjusted to 1.0 to 2.6 V. Cyclic voltammetry was measured at a scan rate of 20 µV s^{-1} between 10 mV and 1 V. The amount of electrolyte was 20 µL in the coin cell, which equates to 12–14 $\mu L_{electrolyte}$ $mg^{-1}{}_{sulfur}$.

All chemicals except for LiTFSI, DME, and DOL were used as received. To remove residual water LiTFSI was dried at 120 °C under vacuum for 24 h before use. DME and DOL were dried and stored over 3 Å molecular sieve.

Characterization: A Siemens D5005 diffractometer (CuKα radiation 0.1542 nm) was used for XRD measurements in an angular range of 2θ = 10–60°. SEM images were acquired with a JEOL JSM-6610LV scanning electron microscope.

Supporting Information

Supporting Information is available from the Wiley Online Library or from the author.

Acknowledgements

We thankfully acknowledge Erik Pflug from Fraunhofer IWS for the DC magnetron sputtering of amorphous silicon.

Received: June 26, 2013
Revised: July 19, 2013
Published online: August 27, 2013

[1] X. Ji, K. T. Lee, L. F. Nazar, *Nat. Mater.* **2009**, *8*, 500.
[2] N. Jayaprakash, J. Shen, S. S. Moganty, A. Corona, L. A. Archer, *Angew. Chem. Int. Ed.* **2011**, *50*, 5904.
[3] B. Zhang, X. Qin, G. R. Li, X. P. Gao, *Energy Environ. Sci.* **2010**, *3*, 1531.
[4] Z. W. Seh, W. Li, J. J. Cha, G. Zheng, Y. Yang, M. T. McDowell, Y. Cui, *Nat. Commun.* **2013**, *4*, 1331.
[5] S. Dörfler, M. Hagen, H. Althues, J. Tübke, S. Kaskel, M. J. Hoffmann, *Chem. Commun.* **2012**, *48*, 4097.
[6] S. Thieme, J. Brückner, I. Bauer, M. Oschatz, L. Borchardt, H. Althues, S. Kaskel, *J. Mater. Chem. A* **2013**, DOI 10.1039/c3ta10641a
[7] M. Oschatz, S. Thieme, L. Borchardt, M. R. Lohe, T. Biemelt, J. Brückner, H. Althues, S. Kaskel, *Chem. Commun.* **2013**, *49*, 5832.

[8] L. Yin, J. Wang, F. Lin, J. Yang, Y. Nuli, *Energy Environ. Sci.* **2012**, *5*, 6966.
[9] Z. Peng, S. A. Freunberger, Y. Chen, P. G. Bruce, *Science* **2012**, *337*, 563.
[10] S. Lu, Y. Cheng, X. Wu, J. Liu, *Nano Lett.* **2013**, *13*, 2485.
[11] W. Li, G. Zheng, Y. Yang, Z. W. Seh, N. Liu, Y. Cui, *Proc. Nalt. Acad. Sci. USA* **2013**, *110*, 7148.
[12] Y. Yang, G. Zheng, Y. Cui, *Energy Environ. Sci.* **2013**, *6*, 1552.
[13] D. Aurbach, E. Pollak, R. Elazari, G. Salitra, C. S. Kelley, J. Affinito, *J. Electrochem. Soc.* **2009**, *156*, A694.
[14] Y. V. Mikhaylik, US 7,354,680 B2, **2008**.
[15] J.-W. Choi, J.-K. Kim, G. Cheruvally, J.-H. Ahn, H.-J. Ahn, K.-W. Kim, *Electrochim. Acta* **2007**, *52*, 2075.
[16] S. S. Zhang, *Energies* **2012**, *5*, 5190.
[17] S. S. Zhang, *Electrochim. Acta* **2012**, *70*, 344.
[18] J. Schuster, G. He, B. Mandlmeier, T. Yim, K. T. Lee, T. Bein, L. F. Nazar, *Angew. Chem. Int. Ed.* **2012**, *51*, 3591.
[19] X. Ji, K. T. Lee, L. F. Nazar, *Nat. Mater.* **2009**, *8*, 500.
[20] G. He, X. Ji, L. Nazar, *Energy Environ. Sci.* **2011**, *4*, 2878.
[21] J. Hassoun, B. Scrosati, *Angew. Chem. Int. Ed.* **2010**, *49*, 2371.
[22] Y. Yang, M. T. McDowell, A. Jackson, J. J. Cha, S. S. Hong, Y. Cui, *Nano Lett.* **2010**, *10*, 1486.
[23] R. Elazari, G. Salitra, G. Gershinsky, A. Garsuch, A. Panchenko, D. Aurbach, *Electrochem. Commun.* **2012**, *14*, 21.
[24] K. Evanoff, J. Benson, M. Schauer, I. Kovalenko, D. Lashmore, W. J. Ready, G. Yushin, *ACS Nano* **2012**, *6*, 9837.
[25] J. Yin, M. Wada, K. Yamamoto, Y. Kitano, S. Tanase, T. Sakaia, *J. Electrochem. Soc.* **2006**, *153*, A472.
[26] V. Etacheri, U. Geiger, Y. Gofer, G. A. Roberts, I. C. Stefan, R. Fasching, D. Aurbach, *Langmuir* **2012**, *28*, 6175.
[27] D. Aurbach, Y. Ein-Eli, O. Chusid, *J. Electrochem. Soc.* **1994**, *141*, 603.
[28] J. K. Lee, K. W. An, J. B. Ju, B. W. Cho, W. I. Cho, D. Park, K. S. Yun, *Carbon* **2001**, *39*, 1299.
[29] F. Böttger-Hiller, P. Kempe, G. Cox, A. Panchenko, N. Janssen, A. Petzold, T. Thurn-Albrecht, L. Borchhardt, M. Rose, S. Kaskel, C. Georgi, H. Lang, S. Spange, *Angew. Chem. Int. Ed.* **2013**, *52*, 6088.
[30] F. Böttger-Hiller, A. Mehner, S. Anders, L. Kroll, G. Cox, F. Simon, S. Spange, *Chem. Commun.* **2012**, *85*, 10568.
[31] F. Orsini, A. Du Pasquier, B. Beaudoin, J. M. Tarascon, M. Trentin, N. Langenhuizen, E. De Beer, P. Notten, *J. Power Sources* **1998**, *76*, 19.
[32] S. Xiong, K. Xie, Y. Diao, X. Hong, *Electrochim. Acta* **2012**, *83*, 78.
[33] Y. V. Mikhaylik, J. R. Akridge, *J. Electrochem. Soc.* **2004**, *151*, A1969.
[34] E. Buiel, J. R. Dahn, *J. Electrochem. Soc.* **1998**, *145*, 1977.
[35] S. Grund, P. Kempe, G. Baumann, A. Seifert, S. Spange, *Angew. Chem.* **2007**, *119*, 636; *Angew. Chem. Int. Ed.* **2007**, *46*, 628.